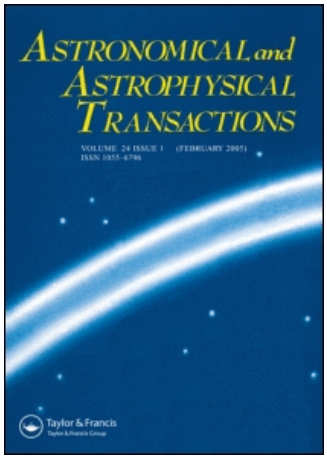

Astronomical & Astrophysical Transactions
The Journal of the Eurasian Astronomical Society
Publication details, including instructions for authors and subscription information:
http://www.informaworld.com/smpp/title~content=t713453505

Interstellar scintillation: observational highlights

B. J. Rickett [a]
[a] ECE Department, University of California, San Diego, CA, USA

Online Publication Date: 01 December 2007
To cite this Article: Rickett, B. J. (2007) 'Interstellar scintillation: observational highlights', Astronomical & Astrophysical Transactions, 26:6, 429 - 439
To link to this article: DOI: 10.1080/10556790701600580
URL: http://dx.doi.org/10.1080/10556790701600580

Astronomical and Astrophysical Transactions
Vol. 26, No. 6, December 2007, 429–439

Interstellar scintillation: observational highlights

B. J. RICKETT*

ECE Department, University of California, San Diego, CA, USA

(Received 19 July 2007)

This paper reviews the chief observational phenomena that define interstellar scintillation (ISS) and have given evidence for a widespread distribution of plasma turbulence on very small scales. Though ISS was discovered in pulsars and is still a major perturbation of their signals, it is now also recognized in a variety of fluctuations in the flux density from quasars and Active Galactic Nuclei (AGNs).

Keywords: Scattering; Scintillation; Interstellar medium; AGN; Pulsars

1. Introduction and history

In the beginning (*i.e.* 1950s), there was scintillation in the ionosphere. This signified both a radio source size smaller than an arc minute and the presence of unexpected substructure in the electron density of the ionosphere. The pioneers in those early investigations were Pisareva, Vitkevich and colleagues here in Russia and Smith, Ratcliffe, Budden and colleagues in the UK. Theoretical work on how a random phase-changing medium can cause amplitude variations (*i.e.* scintillation) was also pursued actively by these investigators and also by Tatarskii *et al.* [1], who drew on the early Russian investigations of turbulence by Kolmogorov [2].

Since that time, interplanetary and interstellar scintillation have been discovered and investigated. These too yield clues on compactness of radio sources and 'micro'-structure in the scattering media. As the distance to the scattering medium increases, so the angular size of a source that cuts off scintillation decreases whereas the relevant length scales probed in the media increase. This review concerns interstellar scintillation and scattering, which was first revealed observationally [3] and analysed theoretically [4, 5] nearly 40 years ago with the discovery of pulsars. In presenting a review, I concentrate on the observed phenomena.

There is an interesting history of how the various scintillation and scattering studies interacted with each other, for which I presented a flow chart [6] at the IAU Colloquium 182 ('Sources and Scintillation', Guiyang, April 2000). The serendipitous discovery of pulsars [7] was intimately related to interplanetary scintillation (IPS) as an unexpected bonus to Tony

*Email: rickett@ece.ucsd.edu

Astronomical and Astrophysical Transactions
ISSN 1055-6796 print/ISSN 1476-3540 online © 2007 Taylor & Francis
http://www.tandf.co.uk/journals
DOI: 10.1080/10556790701600580

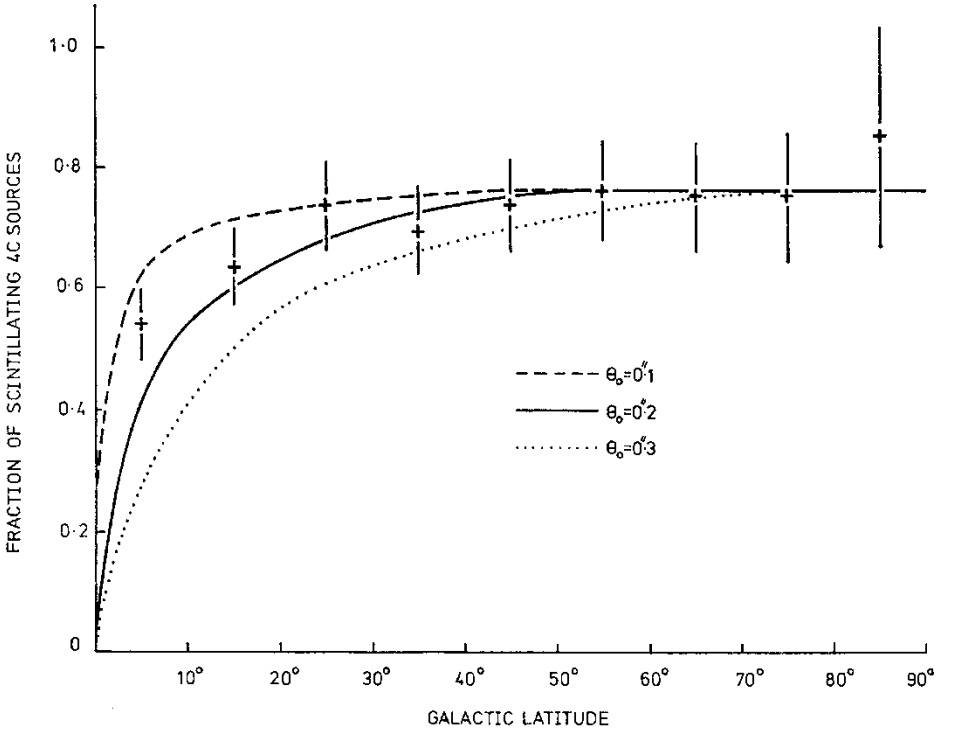

Figure 1. The fraction of 4C radio sources that showed IPS in the Cambridge survey at 81.5 MHz plotted in 10° bins of Galactic latitude [9], with predictions for interstellar angular broadening overplotted.

Hewish and Jocelyn Bell's sky survey at 81.5 MHz for IPS sources. The original goal was to study any cosmological evolution of quasars, which constituted the majority of radio sources small enough in angular size to scintillate (diameters less than about 1 arcsec). As is well known, pulsars were first recognized as an unusual time-variable signal at angles too far from the Sun to be IPS and their discovery became an appendix to Jocelyn Bell's thesis. Their extraordinarily small diameters in turn meant that they showed interstellar scintillation (ISS), since all known radio sources at that time were too large (diameters bigger than about 0.1 milliarcsec). I will discuss ISS for pulsars before the ISS effects that have now been found for some very compact AGNs.

Angular broadening is conceptually the simplest scattering phenomenon. It was detected in the solar wind before IPS was first observed. However, angular broadening in the interstellar medium (ISM) was found some years after ISS was first observed in pulsars. The 81.5 MHz survey [8] from which pulsars were discovered listed IPS observations for 1500 4C sources. The smoothing effect of the source angular diameter was modelled and the inferred diameters exhibited a lower bound of $\sim$0.2 arcsec. Figure 1 [9] shows this as a decrease in the fraction of scintillating sources at low galactic latitudes, with curves indicating the predictions for broadening in the ISM. The interpretation is that all extragalactic sources are broadened by propagating through the irregular ionized ISM. The scattered angle increases at lower latitude due to the increasing path length with a minimum diameter of $\sim$0.2 arcsec at high latitudes. This was the first observational evidence for angular broadening in the ISM.

We now know that we can model the ISM as a turbulent plasma with a Kolmogorov spectrum for which there is a compact theoretical description of the angular broadening. Conveniently for radio astronomers, it is given by a product of the intrinsic source visibility function by the

following factor [10]:

$$V(\boldsymbol{s}) = \exp[-0.5 D_\phi(\boldsymbol{s})] = \exp\left[-0.5\left(\frac{s}{s_\mathrm{d}}\right)^\alpha\right], \quad (1)$$

where $\boldsymbol{s}$ is the interferometer baseline and $D_\phi(\boldsymbol{s})$ the structure function of the cumulated phase along the scattered path. The second equality applies when the electron density has an isotropic wavenumber spectrum following a power law of exponent $-\alpha - 2$, with $\alpha = 5/3$ for the Kolmogorov spectrum, and s_d defines the 'diffractive' scale. This important scale is defined as the lateral separation in the observer's plane over which there is an rms phase difference (computed on a straight line path between the pulsar and the observer) of 1 radian. For a path length L at observing wavelength λ through a uniformly turbulent Kolmogorov medium, one finds that $s_\mathrm{d} \propto \lambda^{-1.2} L^{-0.6}$. Since the scattered brightness function $B(\theta)$ is the Fourier transform of the visibility function, it follows that a point source is broadened to a scattered angular diameter $\theta_\mathrm{scatt} \sim \lambda/(2\pi s_\mathrm{d}) \propto \lambda^{2.2} L^{0.6}$.

2. Pulse broadening

Whereas the angular broadening in the ISM is relatively difficult to detect, there is an associated temporal broadening of pulsar pulses that was already detected from the Crab pulsar in 1970 [11]. Scattered waves that arrive at a *small* angle θ travel further than unscattered waves by an amount that depends on θ^2. Thus, the pulse shape is broadened by a characteristic time $\tau_\mathrm{scatt} \propto \theta^2_\mathrm{scatt}$. This creates the key observational signature of a very steep frequency dependence of the pulse broadening as displayed in figure 2. If we define the scaling by $\tau_\mathrm{scatt} \propto \lambda^x$, one can estimate the exponent α of the density spectrum from $x = 2 + 4/\alpha$. Figure 2 shows a single pulsar observed at 5 frequencies and the range of exponents x estimated from all pulsars with suitable multifrequency observations.

The relationship between angular and temporal broadening is particularly simple for the case when the scattering is concentrated in a thin layer [13]. Modelling this as a screen at distance z_o from the observer and z_p from the pulsar, we find the pulse broadening function to be:

$$P(\tau) = \int_0^{2\pi} \frac{B(\theta = \sqrt{2c\tau/z_e}, \beta)\mathrm{d}\beta}{2\pi} \quad (2)$$

Here $z_e = z_o z_p / L$ with $L = z_o + z_p$ being the pulsar distance. When the scattering is in addition circularly symmetric (as in a medium with statistically isotropic inhomogeneities), the brightness function is independent of the azimuth angle β and there is a direct mapping from arrival time to angle $P(\tau) = B(\theta = \sqrt{(2ct/z_e)})$.

The intrinsic pulse shape convolves $P(\tau)$ to give the observed pulse shape. So, in order to estimate $P(\tau)$, one must first estimate the intrinsic shape from observations at frequencies high enough to be unaffected by scattering and extrapolate any frequency dependence of that shape to the lower frequencies dominated by interstellar broadening. Estimates of the brightness function $B(\theta)$ in turn allow us to constrain the power spectrum of the inhomogeneities in electron density. The scattered pulse shape from PSR J1644-45 was observed at Parkes at 660 MHz and compared with theory [14] for an isotropic Komogorov spectrum with various 'inner scales' that cut off the turbulent cascade at high wavenumbers. Theoretical shapes were shown for a screen and for an assumed uniformly scattering medium, and inner scales of about 100 km were deduced.

When the scattering is anisotropic, such as due to the presence of a mean local magnetic field, the integral over angle β in equation (2) alters the pulse shape. For an anisotropic

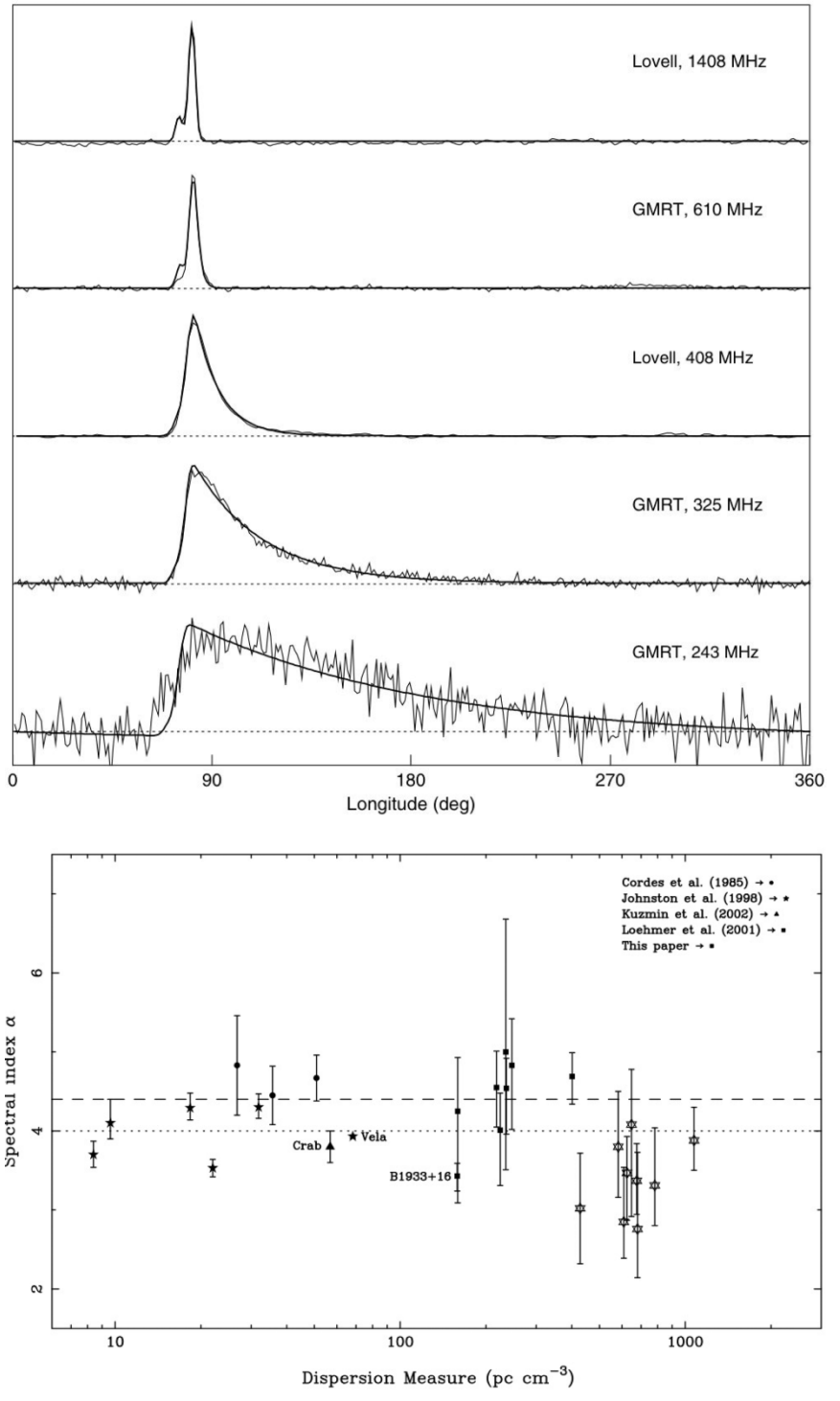

Figure 2. *Left*: profiles of pulsar B1831-03 at 5 radio frequencies from Lohmer *et al.* [12]. The rapid asymmetrical increase in the width $\tau_{\rm scatt}$ with lower frequency is easy to see. *Right*: the wavelength scaling 'spectral index' x plotted against the dispersion measure of each pulsar observed. The expected Kolmogorov value $x = 4.4$ is shown by the dashed line. Note that there are several pulsars for which $x < 4$, which is below the lowest value allowed according to simple theories.

Gaussian brightness function [14], one finds that the far out pulse decay is much slower than the exponential funtion that applies for an isotropic Gaussian brightness. The consequence is that, if we allow the possibility of anisotropic scattering, the inner scale deduced for PSR J1644-45 must be a lower limit.

3. Pulsar scintillation

Pulsar observers fold the received intensity according to the known period and create an average pulse profile averaged over tens of seconds. The associated pulse amplitude is then estimated by setting an off-pulse baseline and finding the mean flux density above that baseline. ISS, displayed as a dynamic spectrum $S_1(\nu, t)$, is seen as deep variations in this amplitude over times on the order of minutes, which are decorrelated over frequency intervals on the order of kilohertz to megahertz (see the left panel of figure 3. The autocorrelation of $S_1(\nu, t)$ along the time and frequency axes, respectively, are used to define characteristic time scales and frequency scales for ISS. Paradoxically, conventions have arisen such that a decorrelation to 1/e is used to define the time scale t_d and decorrelation to 0.5 is used to define the frequency scale ν_d. These quantities are referred to as the diffractive ISS parameters and are readily observed for every pulsar. They are tabulated in the very valuable Parkes pulsar data base (http://www.atnf.csiro.au/research/pulsar/psrcat), with the diffractive frequency scale represented by $\tau_\mathrm{scatt} = (2\pi\nu_d)^{-1}$ scaled to 1 GHz under the assumption that $x = 4.4$.

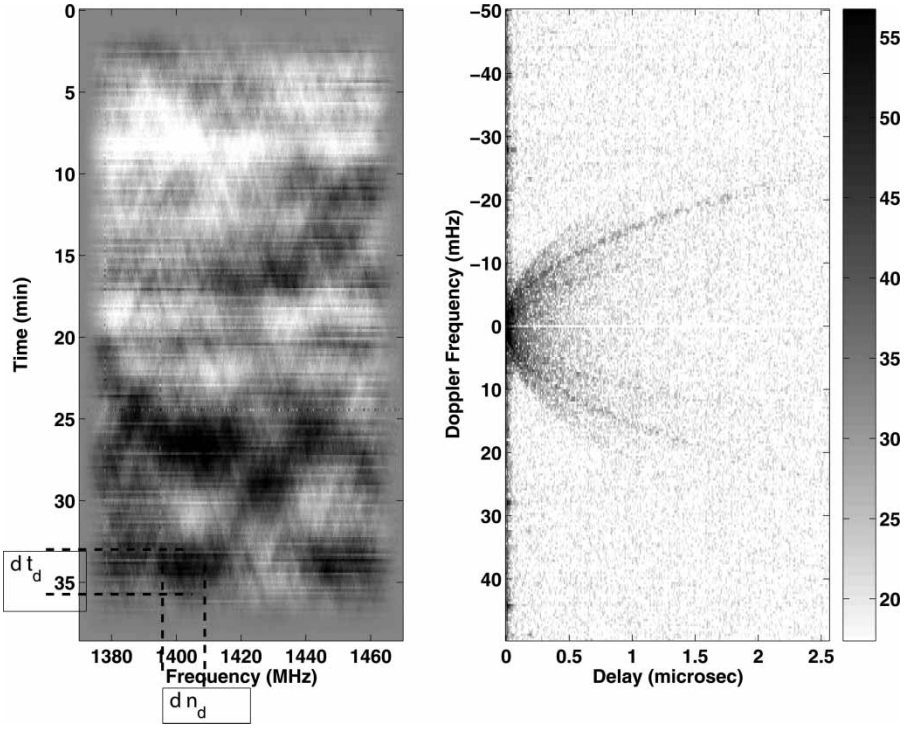

Figure 3. *Left*: dynamic spectrum of PSR B1133 + 16 recorded by Stinebring at Arecibo on modified Julian Date 53224; the darkness of the grayscale is linear in intensity. *Right*: the secondary spectrum (S_2) of the data on the left (its 2-D Fourier power spectrum). The grayscale is logarithmic (dB) as shown in the tablet, revealing three remarkable fine parabolic arcs visible out to large delays.

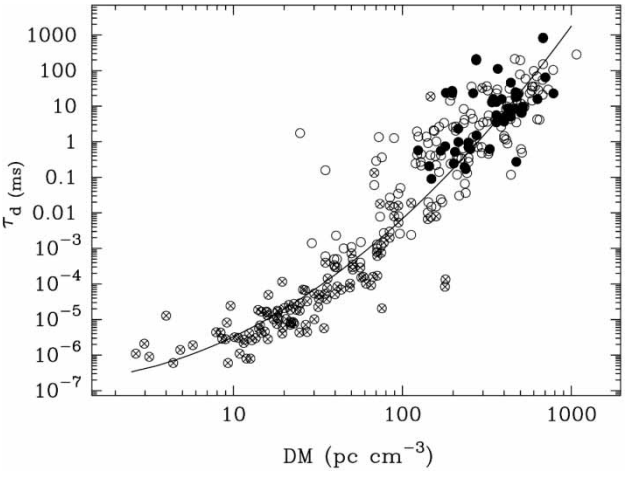

Figure 4. Measurements of $\tau_{\rm scatt}$ scaled to 1 GHz plotted against Dispersion Measure (DM) for each pulsar [15]. The circles with crosses were obtained from the observed ISS decorrelation frequency and the others are $\tau_{\rm scatt}$. Filled circles come form the Arecibo observations [15].

This reciprocal relation between $\tau_{\rm scatt}$ and $\nu_{\rm d}$ results from the fact that ISS imposes a random variation in the received pulse spectrum $S_1(\nu, t)$, which is constant for times shorter than $t_{\rm d}$. The deep modulations in the spectrum (on scale $\nu_{\rm d}$) have an associated impulse response given by the ν-Fourier transform of $S_1(\nu, t)$ at a particular time t. This impulse response, whose ensemble average would be $P(\tau)$, broadens the emitted pulse shape. Its width in time has a reciprocal relation to the width in frequency as for any Fourier transform pair.

Figure 4 shows ISS observations assembled by Bhat *et al.* [15] of $\tau_{\rm scatt}$ plotted against each pulsar's DM. The overlying line is a smooth curve that approximates their relationship. The original evidence for ISS [3] came from such a plot (for $\nu_{\rm d}$) for only 10 pulsars. The expected relation for a uniformly distributed Kolmogorov medium is $\tau_{\rm scatt} \propto DM^{2.2}$, which is a reasonable representation of the trend over $3 < {\rm DM} < 30\,{\rm pc/cm^3}$. However, it greatly underestimates the smooth curve as DM increases, as already noted in 1971 [16].

The conclusion from this discrepancy is that the distant high DM pulsars, which are concentrated at low Galactic latitudes toward the inner Galactic, are seen through an increasingly turbulent medium. $\tau_{\rm scatt}$ responds to the column density of variance in electron density and is closely related to its emission measure. Specifically, the discrepancy requires that the ratio of rms density to mean density increases, which suggests a patchy distribution of highly turbulent plasma with a volume fraction that *decreases* toward the inner Galaxy. Cordes and Lazio [17] represented this in their comprehensive model for the distribution of electrons in the Galaxy by a 500-fold increase in their 'turbulence' parameter. Boldyrev and Gwinn [18] represented the effect by a random spatial distribution that follows Lévy flight statistics rather than Gaussian statistics. Under such statistics, a long scattered path has an increasing probability of intersecting one of the rare extremely turbulent regions. A troublesome aspect of their model is that neither the mean nor the variance of the process can be defined, nevertheless it may well be useful in modelling how distant scattering often appears to be due to a few strongly scattering layers rather than a uniform distribution of scattering along the path.

Just as diffractive ISS (DISS) was first distinguished from intrinsic pulsar variations by the DM dependence of $\nu_{\rm d}$, the phenomenon now called refractive ISS was first recognized by the DM dependence [19] of the time scale of the amplitude variations observed on much longer

time scales (*i.e.* days) [20, 21]. Rickett *et al.* [22] identified the phenomenon of refractive interstellar scintillation (RISS) as causing the observed increase in time scale for more distant pulsars. It should be noted that Rumsey's theoretical investigation of scintillation gave the essential insight into this phenomenon. The spatial scale of the RISS intensity pattern (s_r) is imposed by the typical spatial scale of the scattering disk (or tube), which has a radius of about $s_r \sim L\theta_{scatt}$ for scattering at distance L. Since both L and θ_{scatt} tend to increase with DM, the time scale for RISS increases strongly with DM as observed. Stinebring *et al.* [23] subsequently observed RISS in a five-year program of daily observations at Green Bank. These observations found that the wavenumber spectrum of electron density can be accuratley modelled by a Kolmogorov spectrum; for 15 of the 21 pulsars observed, there was no evidence for an inner scale, while six of them could be modelled by an inner scale cut-off at $\sim 10^{10}$ cm or by a change in the power law exponent of scales 1000 times larger.

Figure 3 shows in the left panel the primary dynamic spectrum of PSR B1133 + 16 at 1420 MHz recorded at Arecibo. One can recognize the characteristic widths ($\nu_d \times t_d$), but with sufficiently fine resolutions one can also see a criss-cross patterned substructure. The right panel shows its Fourier power spectrum (secondary spectrum) plotted *logarithmically* versus delay f_ν (μsec) and frequency f_t (mHz). The remarkable parabolic arcs (first discovered by Stinebring *et al.* [24]) extend well beyond τ_d in delay, albeit at quite low levels. In this example, one can see three parabolic arcs.

The parabolic arcs can be explained as due to the interference of pairs of components in the scattered brightness by $\boldsymbol{\theta}_1$ and $\boldsymbol{\theta}_2$. These components have differing delays and differing Doppler shifts due to their changing path lengths. While the delay depends on the square of the angles $z_e(\theta_1 - \theta_2^2)^2/2c$, the difference in Doppler shifts depends linearly on the angles, giving $f_t = \boldsymbol{V}(\boldsymbol{\theta}_1 - \boldsymbol{\theta}_2)/(\lambda)$, where $\boldsymbol{V}$ is the 'scintillation velocity' relative to the medium [24–26]. These linear and quadratic dependencies give a general quadratic relation between f_t and f_ν.

In the special case that one of the angles is close to zero and $\boldsymbol{\theta}_1 = (\theta_{x1}, \theta_{y1})$, the quadratic becomes a parabola $f_\nu = af_t^2 + b$, where $a = z_e\lambda^2/(2cV^2)$. If $\boldsymbol{V}$ is along the x-axis, $b \propto \theta_{y1}^2$ that is positive, and hence S_2 falls to zero outside the primary arc $f_\nu = af_t^2$. Moreover in such a case, any point (f_ν, f_t) inside that arc can be mapped to the scattered brightness distribution $B(\theta_s, \beta)$, as $\theta_s = \sqrt{(2cf_\nu/z_e)} = (\lambda/V)\sqrt{(f_\nu/a)}$ and $\cos\beta = f_t\sqrt{(a/f_\nu)}$. Thus, we have the remarkable result that an observation of the secondary spectrum with a single antenna can be mapped to the 2-D scattered brightness (since only $\cos\beta$ is determined, points at $\pm\beta$ are superimposed) – under the condition that there is an undeviated wave interfering with an angular spectrum of scattered waves.

The mapping is such that S_2 is greatest for waves from near $\beta = 0$ or π, which brightens the outer edge of the arc. It also means that thin bright arcs occur when the scattering is anisotropic and aligned with the velocity. In figure 3, the most prominent arc is quite narrow as if due to anisotropy, whereas the arc that lies outside it has a filled interior, suggesting a more isotropic scattering at its distance (presumably nearer to the pulsar).

The special case of a strong undeviated component arises directly in weak scintillation, where there is an essentially unscattered 'core' that interferes with the scattered waves. The other case is in strong scintillation from a medium with a power law spectrum (like the Kolmogorov spectrum); then waves within the half-power width of the ensemble averaged scattered brightness act as the core and interfere with an effective 'halo' of waves from much higher angles. The mapping described above is robust in weak scintillation but only applies approximately in strong scintillation under conditions that approach an ensemble average, and then the effective resolution is set by the scattered core. This is distinct from the inversion technique of Walker and Stinebring [27], who attempted to estimate B under snapshot conditions.

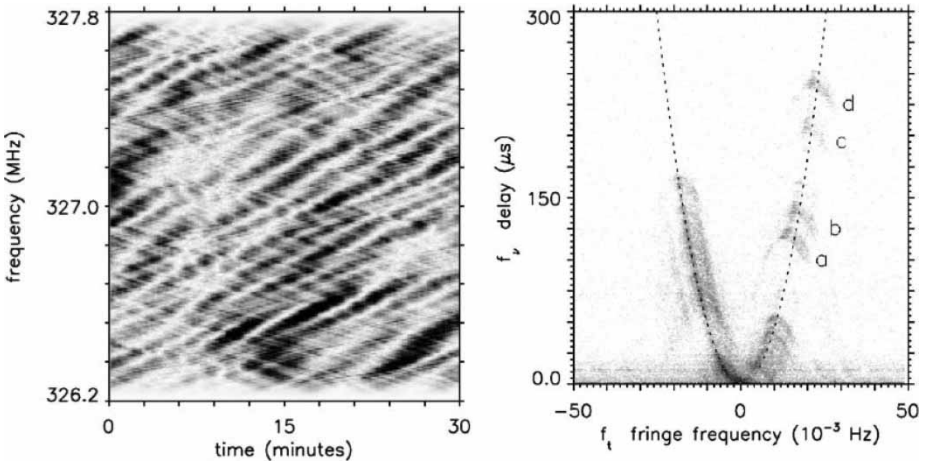

Figure 5. *Left*: dynamic spectrum of PSR B0834 + 06 recorded near 327 MHz by Stinebring at Arecibo in January 2004; the darkness of the grayscale is linear in intensity. *Right*: the secondary spectrum (S_2) of the data on the left. The grayscale is logarithmic in power and covers a total range of $\sim 10^5$ from the maximum power to the noise level. A primary arc fitted to the left side of the main parabola is shown with a dashed line. Numerous inverted parabolas, or arclets, are present with vertices near the primary arc. The four isolated arclets are labelled. Note that the axes in this figure are rotated 90° relative to those in figure 3.

Not only are the parabolic arcs a powerful tool for investigating the wavenumber spectrum and anisotropy of the plasma density, they also reveal information about its distribution along the line of sight, as for example in the multiple arcs in figure 3. An even more remarkable result is shown in figure 5 from Hill *et al.* [28]. As described by Stinebring in these proceedings, observations he has made at Arecibo from PSR B0834 + 06 yield scintillation arcs with detailed substructure. These take the form of 'reverse arclets', in that each is a small fragment of a parabola with its apex lying near the main parabola and having a reversed curvature but with about the same magnitude. There are four particularly obvious examples (a–d) in the figure.

Their analysis [28] suggests that the plasma structures responsible are smaller than an AU in extent and scatter the waves by an angle of $\sim$10 milliarcsec at 327 MHz and have several puzzling features. Their scattering appears to be anisotropic that suggests an origin in sheets or filaments. The inferred electron densities are 10–100/cm^{-3}, which implies a pressure much larger than the ambient warm ISM. The frequency dependence of these features requires an origin at a particular location that does not follow the scaling expected for frequency-dependent refraction. At present, there is no consensus on what these are physically.

4. Quasar scintillation

The influence of ISS on extra-galactic radio sources is largely suppressed by the smoothing that comes from the super-position of diffraction patterns from independently emitting regions extended over the core of the galaxy or quasar. Chashei and Shishov [29] presented the theory of how the source diameter suppresses scintillation and changes its correlation over frequency. In the context of a screen model, relations can be written down simply for the critical source radius that suppresses each regime of scintillation. The source angular radius projected onto the diffraction pattern (at distance L) blurs the pattern over a scale $L\theta_{\rm source}$; when this becomes comparable with the spatial scale of the scintillations, they are partially suppressed and the

fluctuation time is determined by $L\theta_{\rm source}/V$. As a consequence, there are effective cut-off diameters for the three regimes of scintillation:

$$\theta_{\rm diss} = \frac{s_{\rm d}}{L}, \tag{3}$$

$$\theta_{\rm riss} = \frac{s_{\rm r}}{L} = \theta_{\rm scatt}, \tag{4}$$

$$\theta_{\rm weak} = \frac{r_{\rm f}}{L}. \tag{5}$$

Here the weak scintillation regime applies at higher radio frequencies, where the diffractive scale $s_{\rm d}$ is greater than the Fresnel scale $r_{\rm f} = \sqrt{(L\lambda/2\pi)}$ at the typical distance L through the Galactic scattering plasma. In weak ISS (WISS) even a point source has a scintillation index (rms/mean) <1, and the refractive and diffractive regimes merge into one with a spatial scale of $r_{\rm f}$. Since extragalactic sources are often observed at higher frequencies than used for pulsars, they are often observed in moderate or weak scintillation. When $\theta_{\rm source}$ exceeds these limits, the corresponding scintillations decrease inversely with $\theta_{\rm source}$.

Figure 6 approximates the critical diameters for quenching RISS, DISS and WISS for a source at 45° Galactic latitude assuming a scale height of 500 pc. Even the smallest diameter nucleus of an AGN (brightness temperatures 10^{12}–10^{13} K) has an angular extent greater than that of pulsars and so blurs out the DISS, see results claimed for quasar J1819 + 385 [30]. Since RISS has a less stringent limit ($\theta_{\rm riss} \gg \theta_{\rm diss}$), it causes several forms of flux density variability, previously thought to be intrinsic to the sources. 'Low frequency variable' radio sources (*i.e.* year long variations at 200–400 MHz) can be explained as RISS [22, 31, 32]. Flicker over days and intraday variations (IDV) at frequencies of 3–8 GHz can be explained as ISS at the border between WISS and RISS [33–36].

While these studies concentrated on sources with scintillation indices of a few percent, a much higher level of rapid variations has been detected in quasars B0405-385 [37], J1819 +

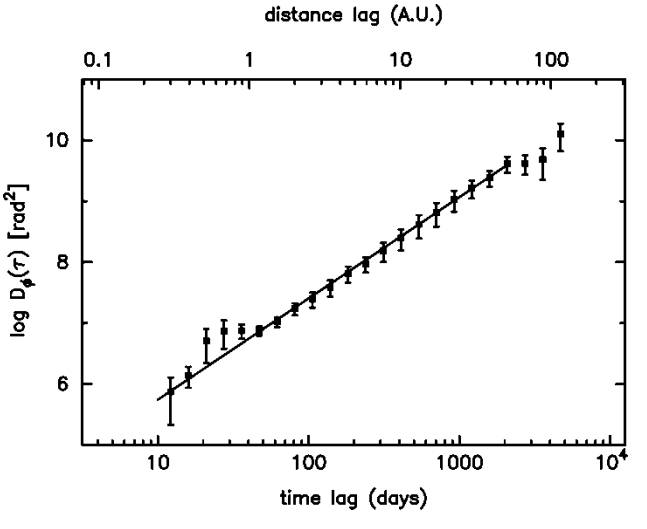

Figure 6. Source diameter plotted versus observing frequency. The dashed lines show source components that are limited by their brightness temperature where $T_b/S_{\rm Jy}$ is the indicated constant. The solid lines are the approximate critical diameters for the three regimes of ISS, for observing at Galactic latitude of 45°. A source component will scintillate like a point source if it lies below the appropriate line. If it lies above the line, its scintillation index will be suppressed by the factor $\theta_{\rm crit}/\theta_{\rm source}$. In which case, the time scale of the appropriate scintillation will be very approximately given by the scale on the right.

385 [38] and B1257-326 [39]. These sources also show annual variation in the characteristic time-scale and have also shown time delays in the variations recorded on intercontinental baselines [40–42]. These characteristics solidly confirm that the variations are not intrinsic to the sources but are due to ISS and so settle a long-running debate.

A new observational search for IDV sources has been completed using the VLA at 6 cm. Lovell *et al.* [43] published results from the first of four epochs of the MASIV survey. Subsequent analysis [44] has shown that about half of the 482 flat spectrum radio sources studied varied at the level of a few percent on a time scale of 2 days or less in two or more epochs. This has interesting consequences for the radio sources themselves, which are thought to be beamed from relativistic jets emanating from AGNs. There is a valuable new theoretical tool for analysing such data in the computations of Goodman and Narayan [45]. These authors have computed the scintillation index, spatial scale, and decorrelation bandwidth for scintillation due to a thin layer through the transition from weak to strong scintillation illuminated by an extended radio source. Thus for those observations where a screen model is appropriate, quantitative interpretation is possible in the regime including the transition from weak to strong scintillation. This is important because theoretical expressions for these quantities are only possible in the appropriate asymptotic limits.

With an ISS explanation for the variations, extreme source brightness temperatures are no longer necessary, and most source structures can now be fitted into the scenario of emission from relativistic jets with Doppler factors consistent with observed 'super-luminal' motion. Possible exceptions exist for the very rapid IDV sources 0405-385 and $1819 + 385$, which we could really call intra-hour variables (IHV). This question depends critically on the distance to the interstellar scattering plasma responsible. All recent attempts [30, 46, 47] to model IHV quantitatively have determined that the responsible plasma turbulence is located in the very local ISM at distances of 1–50 pc, from which the implied brightness temperature is greatly decreased. Thus, it appears that what is unusual about these sources is that they are viewed through unusual local regions that are extremely turbulent.

5. Unsolved puzzles

I will conclude by listing some of the puzzles in the field of ISS that remain unsolved.

- What is the nature of the plasma structures that are concentrated toward the inner Galaxy that cause the upturn in the plot of figure 4 at large DMs? The structures appear to be relatively compact and distributed quite sparsely.
- Do these structures cause anisotropic scattering, which would indicate the dominance of magnetic fields in the fine structures probed by ISS? There is increasing evidence for anisotropy in specific cases of ISS, but our community still models it by isotropic scattering.
- How to explain the observed frequency scaling [12] of the pulse broadening times in which $x < 4$?
- What is the nature of the plasma structures responsible for the 'reverse arclets' reported by Hill *et al.* [28]?
- What physical structures in the local ISM cause the scattering in the few rapid (IHV) scintillating sources.

Acknowledgements

I thank the organizers and Pushchino Radio Astronomy Observatory for arranging this symposium and for their hospitality. I thank the US NSF for support under grant AST 0507713.

References

[1] V.I. Tatarskii, A.S. Gurvich, M.A. Kallistratova *et al.*, Soviet Astron. **2** 578 (1958).
[2] A.N. Kolmogorov, Compt. Rend. (Doklady) Acad. Sci. URSS **30** 301 (1941).
[3] B.J. Rickett, Nature **221** 158 (1969).
[4] P.A.G. Scheuer, Nature **218** 92 (1968).
[5] E.E. Salpeter, Nature **221** 31 (1969).
[6] B.J. Rickett, Astrophysics and Space Science, **278** 5 (2001).
[7] A. Hewish, S.J. Bell, J.D.H. Pilkington *et al.*, Nature **217** 709 (1968).
[8] A.C.S. Readhead and A. Hewish, Mem. Roy. Astron. Soc. **78** 1 (1974).
[9] P. Duffett-Smith and A.C.S. Readhead, MNRAS **174** 7 (1976).
[10] J.A. Ratcliffe, Rep. Prog. Phys. **19** 188 (1956).
[11] J.M. Rankin, J.M. Comella, H.D. Jr. Craft *et al.*, Astrophys. J. **162** 707 (1970).
[12] O. Löhmer, D. Mitra, Y. Gupta *et al.*, Astron. Astrophys. **425** 569 (2004).
[13] W.M. Cronyn, Science **168** 1453 (1970).
[14] B.J. Rickett, Chinese J. Astron. Astrophys. (2005), Chinese Journal of Astronomy and Astrophysics, Suppl. 6, 197.
[15] N.D.R. Bhat, J.M. Cordes, F. Camilo *et al.*, Astrophys. J. **605** 759 (2004).
[16] J.M. Sutton, MNRAS **155** 51 (1971).
[17] J.M. Cordes and T.J.W. Lazio, Astrophys. J./0207156 (v3) (2005).
[18] S. Boldyrev and C.R. Gwinn, Astrophys. J. **584** 791 (2003).
[19] W. Sieber, Astron. Astrophys. **113** 311 (1982).
[20] D.J. Helfand, L.A. Fowler and J.V. Kuhlman, Astron. J. **82** 701 (1977).
[21] T.W. Cole, H.K. Hesse and C.G. Page, Nature **225** 712 (1970).
[22] B.J. Rickett, W.A. Coles and G. Bourgois, Astron. Astrophys. **134** 390 (1984).
[23] D.R. Stinebring, T.V. Smirnova, T.H. Hankins *et al.*, Astrophys. J. **539** 300 (2000).
[24] D.R. Stinebring, M.A. McLaughlin, J.M. Cordes *et al.*, Astrophys. J. **549** L97 (2001).
[25] J.M. Cordes, B.J. Rickett, D.R. Stinebring *et al.*, Astrophys. J. **637** 346 (2006).
[26] M.A. Walker, D.B. Melrose, D.R. Stinebring *et al.*, MNRAS **354** 43 (2004).
[27] M.A. Walker and D.R. Stinebring, MNRAS **362** 1279 (2005).
[28] A.S. Hill, D.R. Stinebring, C.T. Asplund *et al.*, Astrophys. J. **619** L171 (2005).
[29] I.V. Chashei and V.I. Shishov, Sov. Astron. **20** 13 (1976).
[30] J.-P. Macquart and A.G. de Bruyn, Astron. Astrophys. **446** 185 (2006).
[31] N.Y. Shapirovskaya, Sov. Astron. **22** 544 (1978).
[32] B.J. Rickett, Astrophys. J. **307** 564 (1986).
[33] D.S. Heeschen and B.J. Rickett, Astron. J. **93** 589 (1987).
[34] A. Quirrenbach, A. Witzel, T.P. Kirchbaum *et al.*, Astron. Astrophys. **258** 279 (1992).
[35] B.J. Rickett, A. Quirrenbach, R. Wegner *et al.*, Astron. Astrophys. **293** 479 (1995).
[36] B.J. Rickett, T.J.W. Lazio and F.D. Ghigo, Astrophys. J. Suppl. **165** 439 (2006).
[37] L. Kedziora-Chudczer, D.L. Jauncey, M.H. Wieringa *et al.*, Astrophys. J. **490** L9-12 [KCJ] (1997).
[38] J. Dennett-Thorpe and A.G. de Bruyn, Astrophys. J. **529** L65 (2000).
[39] H.E. Bignall, D.L. Jauncey, J.E.J. Lovell *et al.*, Astrophys. J. **585** 653 (2003).
[40] J. Dennett-Thorpe and A.G. de Bruyn, Nature **415** 57 (2002).
[41] J. Dennett-Thorpe and A.G. de Bruyn, Astron. Astrophys. **404** 113 (2003).
[42] H.E. Bignall, J.-P. Macquart, D.L. Jauncey *et al.*, Astrophys. J. **652** 1050 (2006).
[43] J.E.J. Lovell, D.L. Jauncey, H.E. Bignall *et al.*, Astron. J. **126** 1699 (2003).
[44] J.E.J. Lovell, D.L. Jauncey, C. Senkbeil *et al.*, presentation at the Workshop on Small ionized and neutral structures in the ISM, NRAO, Socorro, New Mexico (2006).
[45] J. Goodman and R. Narayan, Astrophys. J. **636** 510 (2006).
[46] B.J. Rickett, L. Kedziora-Chudczer and D.L. Jauncey, Astrophys. J. **581** 103 (2002).
[47] A.G. de Bruyn and J.-P. Macquart, presentation at the Workshop on Small ionized and neutral structures in the ISM, NRAO, Socorro, New Mexico (2006).